Numerical study of ion acoustic turbulence

Zhuo Liu

Plasma Science and Fusion Center - Massachusetts Institute of Technology, Cambridge, MA, 02139, USA

Abstract

Ion acoustic instability is a classical phenomenon in a plasma that has been studied for more than 60 years. However, the nonlinear physics that causes ion acoustic turbulence (IAT) is still unclear. There are also few numerical backups for the theories. I study the dynamics of evolution of non-linear state plasmas in a constant external electric field that causes ion acoustic turbulence using a Vlasov-Poisson code. The preliminary results show some consistency with quasi-linear theory when the external electric field is small. IAT creates anomalous resistivity, run-away electrons and high energy ion tail. IAT is stabilized by changing the shape of the electron distribution.

1 Introduction

Ion acoustic instability is a classic instability in plasma. The typical setup for ion acoustic instability is to have hot moving electrons and cold stationary ions. There is a threshold drift velocity of electrons for the instability to occur. The waves absorb energy from electrons and grow. Ion acoustic instability will evolve in to ion acoustic turbulence (IAT) when the wave amplitude is large enough and waves with different wave numbers begin to interact with each other[1].

There are mainly two motivations for me to study IAT. The first one is straight forward. Bychenkov wrote as a conclusion of his review for IAT in 1986 that "We believe that the present-day results on numerical modeling are very poor and the work in this field which is now almost stopped must be continued in order to obtain a more profound understanding of ion-acoustic turbulence."[1] Although the theory of ion acoustic turbulence of a plasma has been developed for for more than 60 years, the nonlinear physics in it has not yet been fully understood. Since the 1990s, relevant research has nearly come to a stop. Furthermore, although a lot of theories were developed, they lack solid numerical backups. The reason for this, as I will discuss later, is the high demand for computational techniques. Therefore, a deeper understanding of IAT with the help of modern computers is needed.

The second motivation comes from magnetic reconnection. Magnetic reconnection is a process that topological rearranges magnetic field converting magnetic energy to plasma kinetic energy, and is widely seen in the evolution of solar flares, coronal mass ejection, and interaction of solar winds with the Earth's magnetosphere[2]. The typical scenario of magnetic reconnection involves a current sheet in the middle. Oppositely directed magnetic field lines are brought together by plasma flows. Frozen flux constraint is broken and magnetic field lines reconnect in the central area as illustrated in Fig. 1. The simplest model was proposed by Sweet-Parker in an MHD plasma where the frozen flux constraint is broken by resistivity.

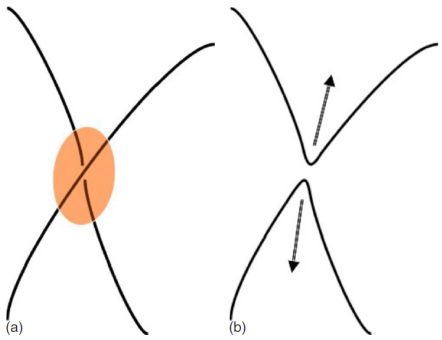

Figure 1: Schematic view of magnetic reconnection[2]

Overall, people are more interested in the reconnection in a collisionless plasma. The reconnection process observed is generally fast compared to theoretical models, and people have been trying to find the reason for fast reconnection. The reconnection rate is tied to the reconnecting electric field, and an electric field is likely to trigger kinetic steaming instabilities, e.g, ion acoustic instability, in current sheets. Moreover, in the reconnecting region, the Ohmic heating is usually going to heat the electrons more, so it is naturally going to develop $T_e > T_i$.

In order to understand reconnection, we need to

know what is balancing the electric field in Ohm's law. When IAT is triggered in a current sheet, parallel electric field will be balanced by the momentum transport from electrons to ions mediated by ion-acoustic waves. In other words, IAT can create anomalous resistivity, which may help to accelerate reconnection process[3, 4]. From the perspective of current sheet formation, IAT may also play an important role because IAT can stabilize current and heat the ions in current sheets. Studying IAT helps us to have a better idea about what kind of reconnection layers we are able to obtain in plasmas, and therefore, help us to understand better the onset of magnetic reconnection. Overall, we should always keep in mind that we never want to study a system that would never exist. Not only should we study the physics from a specific current sheet profile but we should also pay attention to whether we are able to obtain that profile in a real system.

2 Theory of ion acoustic turbulence

2.1 Linear theory

Starting from Vlasov-Poisson Equation,

$$\begin{aligned} \frac{\partial f_\alpha}{\partial t} + v\cdot\nabla f_\alpha - \frac{q_\alpha}{m_\alpha}(\nabla\varphi)\cdot\frac{\partial f_\alpha}{\partial v} = 0 \\ -\nabla^2\varphi = 4\pi\sum q_\alpha\int \mathrm{d}^3 v f_\alpha \end{aligned} \tag{1}$$

where α stands for different species. Follow the standard routine of linear theory, the dielectric function can be written as

$$\begin{aligned} \epsilon(p,k) = \\ 1 - \sum_\alpha \frac{\omega_{\mathrm{p}\alpha}^2}{k^2}\frac{i}{n_\alpha}\int \mathrm{d}^3\boldsymbol{v}\frac{1}{p+i\boldsymbol{k}\cdot\boldsymbol{v}}\boldsymbol{k}\cdot\frac{\partial f_{0\alpha}}{\partial \boldsymbol{v}}, \\ p = -i\omega+\gamma \end{aligned} \tag{2}$$

Given k, one can always choose the x axis to be along k,

$$\epsilon(p,k) = 1 - \sum_\alpha \frac{\omega_{\mathrm{p}\alpha}^2}{k^2}\frac{i}{n_\alpha}\int \mathrm{d}v_x \frac{F'_\alpha(v_x)}{v_x - ip/k} \tag{3}$$

where $F_\alpha(v_x)$ is the 1D distribution function. When $F_\alpha(v_x)$ is Maxwellian, define u and ζ_α: $u = v_x/v_{th\alpha}$, $\zeta_\alpha = ip/kv_{th\alpha}$, $F_{\alpha 0}(v_x) = n_\alpha\left(\frac{1}{\pi v_{th\alpha}^2}\right)^{1/2} e^{-v_x^2/v_{th\alpha}^2}$. Then

$$\begin{aligned} \frac{1}{n_\alpha}\int \mathrm{d}v_x \frac{F'_\alpha(v_x)}{v_x - ip/k} = -\frac{2}{v_{\mathrm{th}\alpha}^2}\left[1+\zeta_\alpha Z(\zeta_\alpha)\right] \\ Z(\zeta) = \frac{1}{\sqrt{\pi}}\int_{-\infty}^{\infty} du \frac{e^{-u^2}}{u-\zeta} \end{aligned} \tag{4}$$

Finally, the dielectric function can be written as

$$\epsilon(p,k) = 1 + \sum_\alpha \frac{1+\zeta_\alpha Z(\zeta_\alpha)}{k^2\lambda_{\mathrm{D}\alpha}^2} \tag{5}$$

where $\lambda_{D\alpha} = v_{T\alpha}/\omega_{p\alpha}$ is the Debye length of certain species. Note that if the Maxwellian distribution has a mean flow, this amounts to a shift by some mean velocity u_α and all one needs to do to adjust the above results is to shift the argument of Z accordingly $\zeta_\alpha \to \zeta_\alpha - u_\alpha/v_{th\alpha}$. Theoretical value of the frequency and growth rate can be obtained by solving

$$\epsilon(p,k) = 0 \tag{6}$$

In the limit $|\zeta_e| << 1$, $|\zeta_i| >> 1$, the growth rate over frequency is

$$\begin{aligned} \frac{\gamma}{\omega} \simeq -\sqrt{\frac{\pi}{8}}\left[\left(\frac{m_e}{m_i}\right)^{1/2}\left(1-\frac{U}{c_s}\right)\right. \\ \left. + \left(\frac{T_e}{T_i}\right)^{3/2}\exp\left(-\frac{T_e/T_i}{2(1+k^2\lambda_{De}^2)}\right)\right] \end{aligned} \tag{7}$$

The threshold drift velocity for instability is

$$U_{th} = c_s(1+\delta_M), \tag{8}$$

$$\delta_M = \left(\frac{m_i}{m_e}\right)^{1/2}\exp\left(-\frac{T_e/T_i}{2(1+k^2\lambda_{De}^2)}\right) \tag{9}$$

δ_M stands for contribution from ions. As ions are much colder than electrons, δ_M is usually negligible. Now taking the external electric field into account. As ion is heavy, the time for the system to reach marginal instability is approximately

$$t_{th} \simeq m_e U_{th}/eE \equiv 1/\nu_{th} \tag{10}$$

As long as ion temperature is low during the evolution, we can ignore the contribution from ions ($\delta_M \ll 1$). So $\gamma \simeq \sqrt{\frac{\pi}{8}}\frac{kc_s}{\sqrt{1+k^2\lambda_{De}^2}}\left(\frac{m_e}{m_i}\right)^{1/2}(u/c_s - 1) \equiv \gamma_s(u/c_s - 1)$. At a time longer than t_{th}, the intensity of IAT grows quadratically

$$\begin{aligned} \sim exp\left(\gamma_s\frac{eE}{m_e c_s}(t-t_{th})^2\right) \\ \simeq exp\left(\frac{(t-t_{th})^2}{2t_{IN}^2}\right), t_{IN} \simeq= \sqrt{\frac{m_e c_s}{2\gamma_s eE}} \end{aligned} \tag{11}$$

t_{IN} characterized the growth rate of the IAT intensity when the mechanism of deceleration of electrons is not yet on. At later time, the deceleration of electrons due to their scattering by IAT pulsations cannot be neglected anymore.

2.2 Quasi-linear theory

The quasi-linear theory is valid when the growing perturbations start modifying the equilibrium before they saturate nonlinearly. This implies that the external electric field cannot be too large. Otherwise, the growth of electron velocity will be much faster than the development of IAT ($t_{th} \ll t_{IN}$). Electrons will be accelerated to very high velocity and it will take a much longer time to stabilize the electrons. Then pulsation of IAT will have enough time to grow to a stage where nonlinear scattering of the waves cannot be neglected. I will briefly talk about this threshold electric field later.

Starting again from Vlasov equation, if we look for the evolution of equilibrium distribution function by averaging over a time period t which satisfies $\omega \ll t^{-1} \ll \gamma$ (This assumes that the quasi-linear variation of electron distribution is slow compared to oscillation and fast compared to the growth of the wave. This is also the situation when quasi-linear theory works), then we can find the equilibrium distribution function evolution equation.

$$\frac{\partial f_0}{\partial t} = \frac{eE}{m_e} F_e'(v) + \frac{e}{m} \int \frac{d\boldsymbol{k}}{(2\pi)^3} i\delta\phi_{\boldsymbol{k}}^* \boldsymbol{k} \cdot \frac{\partial \delta f_{\boldsymbol{k}}}{\partial \boldsymbol{v}} \quad (12)$$

$\delta f_{\boldsymbol{k}}$ is determined from the linear theory

$$\delta f_{\boldsymbol{k}} = i\frac{q}{m} \frac{\delta\phi_{\boldsymbol{k}}}{-i\omega_{\boldsymbol{k}} + i\boldsymbol{k}\cdot\boldsymbol{v} + \gamma_{\boldsymbol{k}}} \boldsymbol{k} \cdot \frac{\partial f_0}{\partial v} \quad (13)$$

Assume that $|\gamma_{\boldsymbol{k}}| \ll |\omega_{\boldsymbol{k}} - \boldsymbol{k}\cdot\boldsymbol{v}|$, and use Plemelj's formula

$$\lim_{\varepsilon\to+0} \frac{1}{x - \zeta \mp i\varepsilon} = \mathcal{P}\frac{1}{x-\zeta} \pm i\pi\delta(x-\zeta) \quad (14)$$

The classical quasi-linear equation for electron of ion acoustic instability is written as [1, 5, 6]

$$-\frac{eEv}{T_{\rm e}} F_{\rm e}(v) = \frac{\partial}{\partial v_i} D_{ij}^{(\rm e)} \frac{\partial}{\partial v_j} f_{\rm e}(\boldsymbol{v}),$$
$$\text{where } D_{ij}^{(e)} = \frac{e^2}{2\pi m_{\rm e}^2} \int {\rm d}k \frac{k_i k_j}{k^2} \frac{\omega_{\rm s}^2}{\omega_{\rm pi}^2} N(\boldsymbol{k}) \delta\left(\omega_{\rm s} - kv\right) \quad (15)$$

ω_s is the sound frequency. $F_{\rm e}$ is the 1D equilibrium Maxwellian electron distribution function. $N(\boldsymbol{k})$ is the number of ion-acoustic quanta multiplied by Planck's constant. This expression comes from the language of quasi-linear particle to describe waves.

$$\frac{N(\boldsymbol{k})}{\hbar} = \frac{|E_{\boldsymbol{k}}|^2}{4\pi\hbar\omega_{\boldsymbol{k}}} \quad (16)$$

$$\frac{\partial N(\boldsymbol{k})}{\partial t} = 2\gamma(\boldsymbol{k}) N(\boldsymbol{k}) \quad (17)$$

Note that following assumptions have been made to arrive at Eq. 15 from Eq. 12: (1) $|\zeta_e| << 1$, $|\zeta_i| >> 1$, so that Eq. 7 is satisfied. (2) $k\lambda_{De} \ll 1$, so that $\omega_s \approx kc_s$. (3) The system has reached a steady state ($\partial/\partial t = 0$). This means that waves do not grow anymore. In other words, we are interesting in the situation when

$$\gamma(\boldsymbol{k}) = \gamma_e(\boldsymbol{k}) - \gamma_{\rm i}(\boldsymbol{k}) = 0 \quad (18)$$

The contribution from ions is just approximately $\delta_M\gamma_s$. The linear growth rate can be calculated by linear theory but with a modified equilibrium distribution function.

$$\gamma_e(\boldsymbol{k}) = -\frac{{\rm Im}\epsilon}{\partial {\rm Re}\epsilon/\partial\omega} = \frac{2\pi^2 e^2}{m_{\rm e}k^2} \frac{\omega_{\rm s}^3}{\omega_{\rm pi}^2} \int {\rm d}\boldsymbol{v}\delta\left(\omega_{\rm s} - \boldsymbol{k}\cdot\boldsymbol{v}\right) \left(\boldsymbol{k}\cdot\frac{\partial f_{\rm e}}{\partial \boldsymbol{v}}\right) \quad (19)$$

$\partial Re\epsilon/\partial\omega = 2\omega_{pi}^2/\omega_s^3$, $Im\epsilon = -(\omega_{pe}^2/k^2)(\pi/n_e)F_e'(\omega/k)$ were used in the derivation of Eq. 17.

Use axially symmetric assumptions, write the intensity of pulsation and electron distribution function as $N(k) = N\left(k, \cos\theta_k\right)$, $f_{\rm e}(v) = f_{\rm Me}(v) + f_{1\rm e}\left(v, \cos\theta_v\right)$,where θ_k, θ_v are the angles between E and k, v respectively. Assume that f_{1e} is small compared to f_{Me}.

From Eq. 15, expand the quasi-linear diffusion operator in spherical coordinates, we can arrive at[1]

$$-\frac{\partial f_{1\rm e}}{\partial\cos\theta_v} = \left[\frac{|e|Ev^3}{2m_{\rm e}c_s v_{T_{\rm e}}^3} + \frac{\nu_1\left(\sin\theta_v\right)}{\sin\theta_v}\right] \frac{c_{\rm s}}{\nu_2\left(\sin\theta_v\right)} \cdot \frac{\partial f_{\rm Me}}{\partial v},$$
$$\nu_n\left(\sin\theta_v\right) = \int \frac{k^3\ {\rm d}k}{4\pi^2} \left(\frac{\omega_{\rm s}}{kv_{\rm s}}\right)^{4-n} \times \int_{-\sin\theta_v}^{\sin\theta_v} \frac{{\rm d}\cos\theta_k}{\sqrt{\sin^2\theta_v - \cos^2\theta_k}} \left(\frac{\cos\theta_k}{\sin\theta_v}\right)^n \frac{\omega_{\rm s} N\left(k, \cos\theta_k\right)}{n_{\rm e}m_{\rm e}v_{T_{\rm e}}} \quad (20)$$

Substitute Eq. 19 and Eq. 20 back into Eq. 18,

$$1 + \delta_{\rm M} - \frac{2}{\pi}\cos\theta_k \times \int_0^{\sin\theta_k} \frac{{\rm d}\cos\theta_v}{\sqrt{\sin^2\theta_k - \cos^2\theta_v}} \frac{v_E + \nu_1\left(\sin\theta_v\right)/\sin\theta_v}{\nu_2\left(\sin\theta_v\right)} = 0,$$
$$\text{where } \nu_E = \sqrt{\frac{9\pi}{8}} \frac{eE}{m_e c_s} \quad (21)$$

Define angular distribution of ion-sound pulsation as

$$\hat{\phi}\left(\cos\theta_k\right) = \int_0^{r_{\rm De}^{-1}} \frac{k^4\lambda_{De}^2\ {\rm d}k}{(2\pi)^2} \frac{\omega_{pi} N(k, \cos\theta_k)}{n_{\rm e}T_{\rm e}} \quad (22)$$

Noting that Eq. 22 actually appears in the integrand of ν_n, Eq. 21 can be re-written as

$$\begin{aligned}&1+\delta_{\mathrm{M}}\\&=\frac{2}{\pi}\cos\theta_k\int_0^{\sin\theta_k}\frac{1}{\sqrt{\sin^2\theta_k-\cos^2\theta_v}}\\&\quad\times\frac{v_E/\omega_{\mathrm{pe}}+\bar{\chi}_1\left(\sin\theta_v\right)/\sin\theta_v}{\bar{\chi}_2\left(\sin\theta_v\right)}d\cos\theta_v\end{aligned}\tag{23}$$

$$\text{where }\bar{\chi}_n(x)=\int_{-x}^{x}\frac{\mathrm{d}x'}{\sqrt{x^2-x^2}}\left(\frac{x'}{x}\right)^n\hat{\phi}\left(x'\right)$$

Eq. 23 can be fulfilled if the following equation is valid

$$\begin{aligned}&\frac{v_E/\omega_{\mathrm{pe}}+\bar{\chi}_1\left(\sin\theta_v\right)/\sin\theta_v}{\bar{\chi}_2\left(\sin\theta_v\right)}=\frac{1+\delta_M}{\sin^2\theta_v}\text{ , or}\\&\frac{\omega_{\mathrm{pe}}}{\nu_E}\left(1+\delta_{\mathrm{M}}\right)\int_0^x\frac{x'\hat{\phi}\left(x'\right)\mathrm{d}x'}{\sqrt{x^2-x'^2}}\left(\frac{x'}{x^2}-\frac{1}{1+\delta_{\mathrm{M}}}\right)=x^2\end{aligned}\tag{24}$$

To solve $\hat{\phi}$, multiply both sides of Eq. 24 by $x(s^2-x^2)^{-1/2}$ and integrate over x from 0 to s, we finally obtain the ion acoustic pulsation spectrum

$$\hat{\phi}\left(\cos\theta_k\right)=\frac{4\nu_E}{3\pi\omega_{\mathrm{pe}}\cos\theta_k}\frac{\mathrm{d}}{\mathrm{d}\cos\theta_k}\left(\frac{\cos^4\theta_k}{1+\delta_{\mathrm{M}}-\cos\theta_k}\right)\tag{25}$$

This is the famous Kovrizhnykh distribution[5, 6]. Finally, anomalous resistivity can be obtained[1].

$$\begin{aligned}&J=e\int\mathrm{d}\boldsymbol{v}\boldsymbol{v}f_{\mathrm{e}}(\boldsymbol{v})\\&J_Z=e\pi\int_0^\infty v^3\,\mathrm{d}v\int_0^\pi\mathrm{d}\theta_v\sin^3\theta_v\frac{\partial f_{1\mathrm{e}}}{\partial\cos\theta_v}\\&J_Z=\sigma E\\&\sigma\simeq\frac{en_{\mathrm{e}}c_{\mathrm{s}}}{E}\left[\frac{3}{2}\left(1-\beta_{\parallel}\right)+\frac{16}{\pi}\beta_{\parallel}\right],\beta_{\parallel}\simeq0.177\end{aligned}\tag{26}$$

2.3 Electric field for reference and nonlinear theory

This part is not the focus of my current research, but I will keep some of my understanding here for reference. Note that the electric field is "weak" even for Alfvenic reconnection. Although how weak exactly the electric field is needs further investigation, there is a general sense that I'm more interested in weak electric fields.

To understand what electric field is "weak" in IAT, one needs to consider nonlinear theory. Taking the induced scattering of the waves of ions into account, the quasi-stationary IAT distribution is determined by

$$\gamma_{\mathrm{e}}(\boldsymbol{k})-\gamma_{\mathrm{i}}(\boldsymbol{k})-\gamma_{\mathrm{NL}}(\boldsymbol{k})=0\tag{27}$$

$$\begin{aligned}&\gamma_{\mathrm{NL}}(\boldsymbol{k})=\\&-\frac{\pi k^2v_{T_{\mathrm{i}}}^2}{n_im_i\partial\omega_{\mathrm{S}}/\partial k}\times\\&\frac{\partial}{\partial k}\frac{k^{-6}}{\partial\omega_{\mathrm{s}}/\partial k}\int\frac{\mathrm{d}\boldsymbol{k'}}{(2\pi)^3}N\left(\boldsymbol{k}'\right)\delta\left(\boldsymbol{k}-\boldsymbol{k'}\right)\left|\boldsymbol{k}\times\boldsymbol{k'}\right|^2\left(\boldsymbol{k}\cdot\boldsymbol{k'}\right)^2\end{aligned}\tag{28}$$

From Eq. 27, we can write the equation very similar as Eq. 23, but taking the nonlinear damping rate (due to induced scattering process) into account,

$$\begin{aligned}&1+\delta_{\mathrm{M}}-\frac{2}{\pi}\cos\theta_k\times\\&\int_0^{\sin\theta_k}\frac{\mathrm{d}\cos\theta_v}{\sqrt{\sin^2\theta_k-\cos^2\theta_v}}\frac{v_E+\nu_1\left(\sin\theta_v\right)/\sin\theta_v}{\nu_2\left(\sin\theta_v\right)}\\&-\frac{k^2v_{Ti}^2}{\gamma_s}\times\\&\frac{\partial}{\partial k}\left[k^4\int_{-1}^1d\cos\theta_{k'}Q(\sin\theta_k,\cos\theta_{k'})\frac{N(k,\cos\theta_{k'})}{4\pi n_eT_e}\right]\\&=0\end{aligned}\tag{29}$$

The same assumptions have been made here. $Q(x,x')$ is a polynomial function of x and x' and is also called the "kernel function" of the nonlinear interaction. $N(k,\cos\theta_k)$, viewing from Eq. 29, can be written in the form of $N(k,\cos\theta_k)=N(k)\Phi(\cos\theta_k)$. $N(k)$ can be estimated by the famous Kadomtsev-Petviashvili spectrum[7]

$$N(k)=\frac{4\pi n_eT_e}{{v_{Ti}}^2}\frac{\gamma_s(k)}{k^5}\ln\frac{1}{kr_{De}}\tag{30}$$

Then Eq. 29 can be simplified, similar to Eq. 23, as

$$\begin{aligned}&1+\delta_{\mathrm{M}}+\int_{-1}^1d\left(\cos\theta_k'\right)Q\left(\sin\theta_k,\cos\theta_k'\right)\Phi\left(\cos\theta_k'\right)\\&=\frac{2}{\pi}\cos\theta_k\int_0^{\sin\theta_k}\frac{1}{\sqrt{\sin^2\theta_k-\cos^2\theta_v}}\\&\quad\times\frac{v_E/\nu_N+\chi_1\left(\sin\theta_v\right)/\sin\theta_v}{\chi_2\left(\sin\theta_v\right)}d\cos\theta_v\end{aligned}\tag{31}$$

$$\text{where }\chi_n(x)=\int_{-x}^{x}\frac{\mathrm{d}x'}{\sqrt{x^2-x^2}}\left(\frac{x'}{x}\right)^n\Phi\left(x'\right),$$

$$v_N=v_{Te}\int\frac{k^2dk}{(2\pi)^2}\frac{\omega_sN(k)}{n_eT_0}=\frac{\omega_{pi}}{\sqrt{8\pi}}\frac{T_e}{T_i}\tag{32}$$

ν_N basically characterizes the rate of the development of nonlinearity, and ν_E, the same as that in quasi-linear theory, characterizes the acceleration rate of electrons by the electric field. The turbulent Knudsen number is defined as

$$K_N=\frac{\nu_E}{\nu_N}=\frac{E}{E_{NL}}\tag{33}$$

$$\text{where }E_{NL}=\frac{m_ec_s\omega_{pi}}{6\pi e}\frac{T_e}{T_i}\tag{34}$$

The value of Knudsen turbulent number is essential in determining the solution of Eq.31, and therefore, IAT dynamics. E_{NL} is an important reference for electric fields. If $E \gg E_{NL}(K_N \gg 1$, strong electric field), the nonlinear induced scattering of waves by ions would be essential in the IAT dynamics just in the first stage of the deceleration of electrons. Therefore, in this situation, Kovrizhnykh distribution (Eq. 25) would never form. In other words, Eq. 25 is valid only for $K_N < 1$.

The last thing I would like to mention here is the famous Saagdev resistivity. When $K_N \gg 1$, by solving Eq. 31 [1]

$$\Phi(x) = \frac{2\sqrt{K_N}}{\pi x^2}\frac{\mathrm{d}}{\mathrm{d}x}\int_0^x \frac{x'^5\,\mathrm{d}x'}{\sqrt{x^2-x'^2}} \times [0.26 - 0.19x'^2 + 0.31x'^4 + x'^2\sqrt{1-x'^2}\left(0.09 - 0.31x'^2\right)\ln\frac{1+\sqrt{1-x'^2}}{x'}]^{-1} \tag{35}$$

Use this spectrum and do a similar calculation as Eq. 26

$$\sigma_{\mathrm{A}} \simeq 0.4\omega_{\mathrm{pe}}\frac{\lambda_{\mathrm{Di}}}{\lambda_{\mathrm{De}}}\left(\frac{8\pi n_{\mathrm{e}}T_{\mathrm{e}}}{E^2}\right)^{1/4} \tag{36}$$

This is the famous Sagdeev anomalous resistivity[8].

2.4 Summary

As one may perceive, the theory of IAT is very complicated. (1) Tons of assumptions have been made. We are in a long wavelength region. And some assumptions made on the velocity might not always be true (For example, ion sound velocity is much larger than ion thermal velocity is not true if ions are well heated). The derivation from Maxwellian can also be very large. (2) The dynamics of ions are completed neglected so far. Ions can also be heated, so the contribution from ions to the damping of waves can also be a complicated function that varies with time instead of the simple δ_M. (3) These theories have assumed quasi-stationary states from the beginning, which might not even be true in a real system (For example, the current does not return to a marginal instability).

3 Simulation setup

I use Gkeyll code. Gkeyll is a computational plasma physics code mostly written in C/C++ and LuaJIT. Gkeyll contains solvers for gyrokinetic equations, Vlasov-Maxwell equations, and Vlasov-Poisson equations. For IAT simulation, I use Vlasov-Poisson solver.

I start with cold Maxwellian ions and hot Maxwellian electrons. I use Cartesian coordinates with two spatial dimensions and two velocity space dimensions. Periodic condition is applied to spatial boundaries. An external electric field is applied to accelerate the electrons and ions. The current gradually ramps up and reaches the threshold for ion acoustic instability. The reason for starting with stable electrons and ions is simple: we do not want to start with a drift velocity that may never be achieved in a real system. This is also understandable from the point of view of onset of reconnection.

Two dimensions both in real space and velocity space are needed. In 1D simulation, ion acoustic instability is switched off by the formation of a small plateau in electron distribution function. In 2D case, the resonance condition is $\boldsymbol{k}\cdot\boldsymbol{v} = \omega$, so a broad spectrum is excited. A plateau cannot stabilize oblique modes, which makes the ion-sound instability more effective. [9]

3.1 Parameters for simulations

3.1.1 Physical parameters

Time is normalized to ω_{pe}^{-1} and length to d_e for simplicity, and therefore, velocity is normalized to c, the light speed. Main physics parameters are

$$v_{Te} = 0.02, \tag{37}$$

$$\frac{m_{\mathrm{e}}}{m_{\mathrm{i}}} = \frac{1}{25}, \tag{38}$$

$$\frac{T_{e0}}{T_{i0}} = 50 \tag{39}$$

The mass ratio is set to be small for faster simulation in the early stage of study on this problem. Small collisions between electron and electron are added for numerical regularization. I hope that the collisions are small enough that this is an insignificant energy loss channel. The other important physics parameters are calculated as $v_{Ti} = 0.00056$, $\omega_{pi} = 0.2$, $\lambda_{De} = 0.02$, $\lambda_{Di} = 0.00283$, $c_s = 0.004$, $E_{NL} \simeq 0.002\frac{en_0 d_e}{\epsilon_0}$.

3.1.2 Spatial box

The boundary of the simulation box is set to be (external electric field is pointed in z direction)

$$(z_{min}, z_{max}) = (0, 1)$$
$$(y_{min}, y_{max}) = (0, 0.5) \tag{40}$$

The resolution can be determined by examining the unstable wavenumbers when the drift velocity of electron is high. If one plots the figure of growth rate versus k, there is a critical wave number k_{crit} where the growth rate goes from positive to negative as it is shown in Fig. 2. The drift velocity is set to be 0.01 ($2.5c_s, c_s = 0.004$) as an example.

The critical wave number for the growth rate to be negative is about $2\pi k_{crit} \approx 16 * 2\pi \approx 100$. Note that Gkeyll is using an interpolation method when running the simulation. The actual number of grids is three times what is set in the input file. Taking simulation efficiency into account, I set

$$\Delta x = \frac{1.0}{32} \tag{41}$$

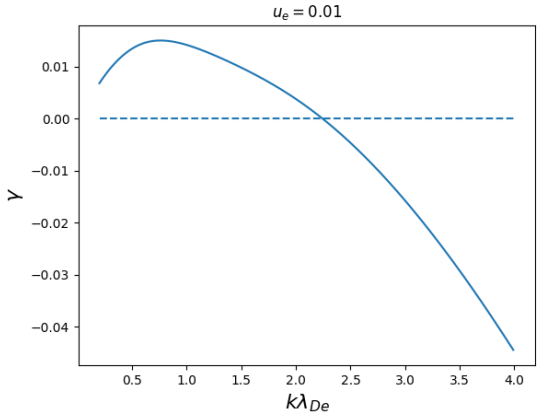

Figure 2: Growth rate versus wave number when electron drift velocity is 0.01

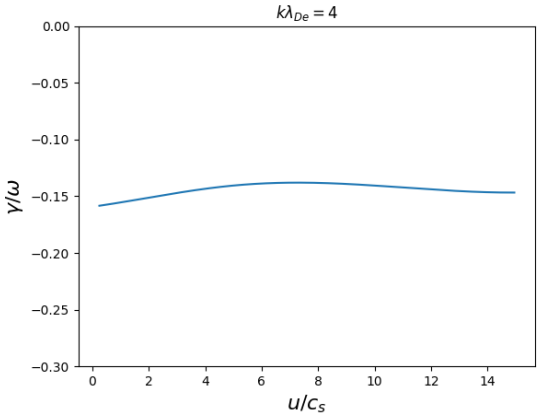

Figure 3: Growth rate versus electron drift when $k\lambda_{De} = 4.0$

In other words, the number of grids in z direction is 32 and 16 in y direction (multiplied by 3 by Gkeyll during simulation). The actually grid size in both directions is $\Delta x_0 = 1/3 * 32$. Please note that the ion Debye length $\lambda_{Di} = v_{Ti}/\omega_{pi} \approx 0.0028 < \Delta x_0$. The grids actually do not resolve ion Debye length well. Although this is fine in the linear stage, there is a concern that not resolving λ_{De} well may affect the simulation in the non-linear stage. However, this setup may actually be reasonable. The reason for an initially strongly damped mode being kept in the simulation is because there would be a nonlinear change in the shape of the distribution functions that would make that mode unstable. However, during the simulation, the ion heating increases the Debye length, which makes the short wavelength waves (high wave number) even more strongly damped. Note that the damping rate of short wavelength modes depends weakly on the drift velocity as it is shown in Fig.3. Therefore, most modes excited in the system are the modes with $k\lambda_{De} \sim 1$. We may not need to care too much about the short wavelength waves.

3.1.3 Electron velocity space

First, what should be the grid size for electron velocity space? This depends on the width of the resonance region in electron velocity space. The width of the resonance region may be estimated as follows. The effective potential energy for a particle moving at speed $\omega_{\boldsymbol{k}}/k + \delta v$ can be written as

$$U(x) = -U_0 \cos(kx) \tag{42}$$

The frequency of oscillation of a trapped particle can be estimated as

$$\omega_{\rm B} = \sqrt{\frac{U_0 k^2}{m}} = \sqrt{\frac{e\delta\varphi_{\boldsymbol{k}} k^2}{m}} = \sqrt{\frac{e\delta E_{\boldsymbol{k}} k}{m}} \tag{43}$$

It is reasonable to estimate that a single mode will saturate if it reaches an amplitude where the bounce frequency is comparable to the linear growth rate:

$$\gamma_{\boldsymbol{k}} \sim \omega_{\rm B,max} \sim \sqrt{\frac{e\delta E_{\boldsymbol{k},\rm max} k}{m}} \implies \delta E_{\boldsymbol{k},\rm max} \sim \frac{m\gamma_{\boldsymbol{k}}^2}{ek} \tag{44}$$

Finally, the trapping width of the saturated wave is given by

$$m\delta v^2 \sim U_{0,\rm max} \sim e\varphi_{\boldsymbol{k},\rm max} \sim \frac{m\gamma_{\boldsymbol{k}}^2}{k^2} \implies \delta v \sim \frac{\gamma_{\boldsymbol{k}}}{k} \tag{45}$$

The largest drift velocity the system can reach when electric field is small is about $u_e \approx 0.01$. Fig. 4 shows γ_k/k versus wave number when electron drift velocity is 0.01. Ideally, I would like to resolve all the unstable modes. It is reasonable to set the grid size to be around 0.001. Based on some numerical experiments, I finally set the grid size to be 1/1200.

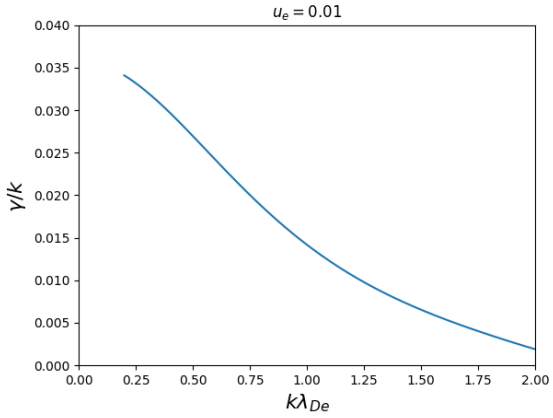

Figure 4: Estimate the resonance width

Second, setting up the electron velocity range is not trivial either. The electron velocity range has to be large enough to hold the entire electron distribution function while it is being accelerated by the electric field and heated by turbulence. Based on some experiments, I set

$$(v_{ez,min}, v_{ez,max}) = (-3.0v_{Te}, 12.0v_{Te}) \tag{46}$$

For the box size in Eq. 46, the number of the grids is

$$N_{v_{ez}} = 120 \tag{47}$$

(46) and (47) are the setup in electric field direction. The y direction is relatively easy and is set to be $(v_{ey,min}, v_{ey,max}) = (-6.0v_{Te}, 6.0v_{Te})$.

I will show in section 5 that there are still some problems with this electron velocity range. The problems are mainly because the lower boundary in z direction $-3v_{Te}$ is not good. This lower boundary will truncate the Maxwellian a little bit, which will lead to numerical instability when the simulation goes long.

3.1.4 Ion velocity space

Setting up an ion velocity simulation box is easier than that of electron. Ions are cold, and have small thermal speed. Ions are also heavy and cannot be accelerated to a very high speed. However, it's still important to make sure that the resonant ions are well resolved as the resonance region for ions is way out in the tail. $v_{Ti} \approx 0.00056$, and $c_s = 0.004$. In the previous PIC simulation [9], ions will form a high energy tail up to $2c_s$. Therefore, the ion velocity range is set to be (in both directions)

$$(v_{i,min}, v_{i,max}) = (-16.0v_{Ti}, 16.0v_{Ti}) \tag{48}$$

$$N_{vi} = 32 \tag{49}$$

3.1.5 Noise

As the simulation proceeds, the system becomes unstable to a progressively broader range of wave numbers. At the same time, there is Landau damping for initially stable (damped) waves. Therefore, only initial perturbation is not enough. We need continual excitation of all waves. I simply inject noise at every time step t_α with a stochastic amplitude and phase:

$$\left(\frac{\partial F^i}{\partial t}\right)_{\text{noise}} = \sum_\alpha \delta(t - t_\alpha) \times \sum_{n_y, n_z \in \mathcal{N}} \chi_0(n_y, n_z) \cos(\boldsymbol{k_n} \cdot \boldsymbol{x} + \phi_{\boldsymbol{n}}(t_\alpha)) \tag{50}$$

I only perturb the ions. This is simply because it is an effective way to excite predominantly the ion-acoustic branch.

3.2 Linear benchmarking

Use the parameters giving above, a group of simulations is done to verify that these parameters indeed can produce correct numerical results at least in the linear stage. In the linear benchmarking simulations, no electric field is applied. The electron distribution is set to be Maxwellian that has unstable drift velocity initially. Only one mode is excited in each simulation. Perturbation is only applied on ions initially. There is no noise throughout the simulations.

The linear benchmarking comprises two parts. The first part is to vary electron drift velocity while keeping the wave number being constant. And the second part is to vary wave number while keeping drift velocity constant. The results are listed in Table 1 and 2.

Table 1: keep $k = 10 * 2\pi$, vary electron drift velocity

$\boldsymbol{u_e}$	γ	γ_{theory}	ω	ω_{theory}
0.005	0.0036	0.0038	0.167	0.170
0.0075	0.0078	0.0080	0.167	0.171
0.01	0.00119	0.0122	0.170	0.172
0.0125	0.00161	0.0162	0.173	0.173
0.015	0.00199	0.0202	0.182	0.176

Table 2: keep $u_e = 0.01$, vary wave number

$\boldsymbol{k/2\pi}$	γ	γ_{theory}	ω	ω_{theory}
10	0.0119	0.0122	0.170	0.172
12	0.0095	0.0097	0.183	0.187
15	0.0053	0.0059	0.208	0.204
18	0.0002	0.0003	0.234	0.224

All the simulation results agree well with the theoretical value. This is a piece of evidence that the choice of simulation parameters is reasonable.

4 Preliminary results

As I stated in Secton 2, I will focus on small electric fields. Electric field in this simulation is $E = 0.00001$ (normalized to $\frac{en_0 d_e}{\epsilon_0}$).

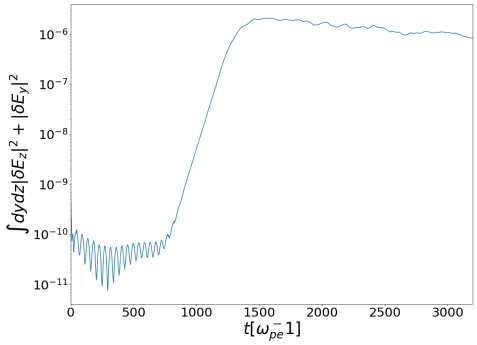

Figure 5: Field energy as a function of time

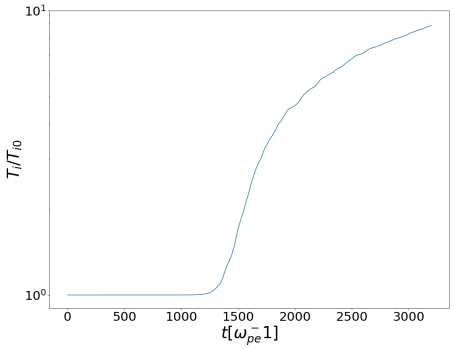

Figure 6: Ion temperature as a function of time

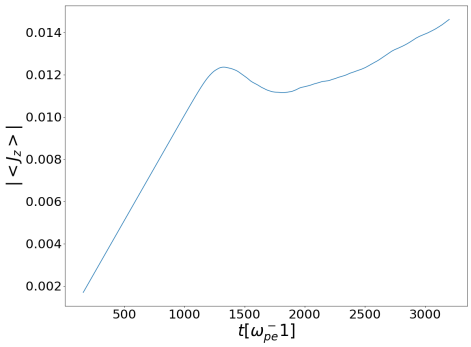

Figure 7: Current as a function of time

As the simulation starts with stationary electron and ions, it is stable in early stage. The field energy is plot in Fig. 5. At around $t = 400\omega_{pe}^{-1}$, the drift velocity of electrons exceeds U_{th} as it was calculated in Eq. 8. The system then becomes unstable, and the waves start to grow linearly. Before $t \approx 800\omega_{pe}^{-1}$, the growth of the waves is described by linear theory. Around $t \approx 900\omega_{pe}^{-1}$, a plateau begins to form in the electron distribution function around the resonance region, and therefore, the field energy grows less and less intensively. During $t \approx 900\omega_{pe}^{-1}$ to $1400\omega_{pe}^{-1}$, this plateau in electron distribution evolves into a new peak and the original peak of the electron distribution disappears. The new peak is located at the resonant area (around U_{th}) and is marginally unstable to ion acoustic instability. In the same time, there is also a high energy tail forming in the electron distribution. The electrons in this tail are not resonant with the wave and are freely accelerated by the electric field. In other words, the electron distribution function after $t \approx 1600\omega_{pe}^{-1}$ can approximately be separated into two groups as illustrated in Fig. 8. In Fig. 8, two Maxwellian functions are used to fit the electron distribution at times later than $1600\omega_{pe}^{-1}$. The bulk of the electron, as stated above, is centered at U_{th} and remains nearly unchanged throughout the remaining of the simulation despite the existence of an external electric field. The tail is freely accelerated by the electric field because the drift velocity of the tail between $t = 2400\omega_{pe}^{-1}$ and $t = 3200\omega_{pe}^{-1}$ differs by $E * \Delta t/m_e, (\Delta t = 800\omega_{pe}^{-1})$. The field energy has nearly reached a steady state after $t \approx 1600\omega_{pe}^{-1}$. The slight decrease is mainly due to the heating of ions.

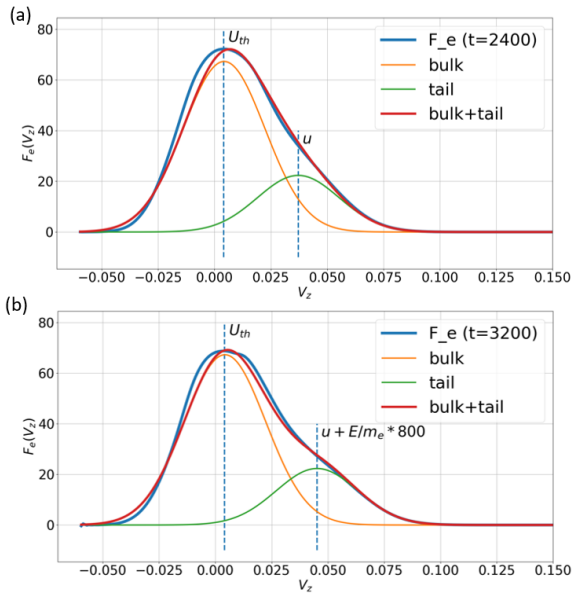

Figure 8: Fit of electron distribution $F_e(v_z)$ with two Maxwellian functions at two different time points. The 1d distribution function is obtained by integrating over the other direction. Bulk is marginally unstable to ion acoustic instability. Tail is freely accelerated by the electric field.

Fig. 7 is the current evolution and is easily understood from the description above (Ions make very little contribution to the current). We can think of it using anomalous resistivity. In a collision less plasma, the current will continuously grow if there is no anomalous resistivity. The effective collision frequency can be estimated using this simple model (assuming ions are heavy and have very

small drift velocity)

$$m_e n_e \frac{du_e}{dt} = e n_e E - \nu_{eff} n_e m_e u_e \tag{51}$$
$$J = e n_e u_e$$

Therefore,

$$\nu_{eff} = \frac{e^2 n_e E/m_e - dJ/dt}{J} \tag{52}$$

This collision frequency is 0 in the linear stage, but remains non-zero throughout the rest of the simulation. After $t \approx 1600\omega_{pe}^{-1}$, instead of returning to marginal instability, the current again begins to increase, and this is because of the high energy electron tail mentioned above. The bulk of the electron remains nearly stationary in the external electric field through the anomalous resistivity. In this sense, the bulk of the electrons satisfies the simple model in the Bychenkov's review [1]. However, the tail is not negligible.

Now let's focus on ions. Nearly at the time of wave saturation, the high energy of the ions starts to form, and ions start to be well heated as plotted in Fig. 6. The formation of high energy ion tail is consistent with what was observed in the previous PIC simulations[9, 10]. However, it was stated there that the quenching of IAT is caused by trapping of ions or formation of high energy ion tail, which I think it's not true. The simulation here shows that the heating of ions plays a minor role. Ions are cold and the contribution to the damping rate is negligibly small. The saturation of IAT is caused by the changing shape of the electron distribution function. Nevertheless, the association of onset of ion heating and saturation IAT is an interesting phenomenon. Qualitatively, there are very few ions absorbing energy from waves in the linear stage because the resonant region is far in the tail for ions. During the quasi-linear relaxation of electrons distribution, there is sudden drop of electron momentum in a short period. And this momentum is transported to ions through the waves due to momentum conservation, which causes much more ions to be resonant with the waves. At time later than $t \approx 1400\omega_{pe}^{-1}$, the ions are heated through Landau damping. Ion distribution is forming a plateau around the resonance region and will probably saturate via quasi-linear relaxation. The simulation needs to run longer to prove this.

Finally, let's examine how the quasi-linear model works. The most important and interesting examination should be checking the anomalous resistivity predicted by Eq. 26. As the current is continuously growing, one may calculate the resistivity using the current at the end of quasi-linear change of electron distribution. This leads to $1/\sigma \approx 0.0009$, which shows some agreement with the theoretical value $1/\sigma_{theory} \approx 0.00011$. Note that Sagdeev resistivity is $1/\sigma \approx 0.026$, which obviously is not a good estimation under this circumstance. This serves as a piece of evidence that quasi-linear model works for very cold ions and a very small electric field. In the study of reconnection with anomalous resistivity, one should be careful about the formula to use. Basically when the electric field is small, Sagdeev resistivity does not apply.

5 Future work

The first thing to resolve is the numerical concerns. As the simulation goes longer, a numerical instability will develop around the lower boundary of z dimension in the electron velocity space. This is because setting the lower boundary to be $-3v_{te}$ will truncate the initial Maxwellian function a little bit. This simulation needs to go longer for better results. Another thing is that $12v_{te}$ is actually a large upper boundary for electron velocity space, which causes some waste of computational resources. This simulation took 8 days running on 128 cores, which is already very expensive. This also explains why there have been few computational works of IAT since the 1980s.

As for the simulation results, they are also a lot of things to explain. Although there is some evidence that shows consistency between the theory and simulation, a more quantitative understanding is needed.

One important consideration comes from the behavior of the ions. First, even if the contribution from ions to the damping of the waves is not important, there is some interesting physics about ions. The simulation results shown above have not come to a completely steady state. Ions are heated in the process. Will it saturate through quasi-linear relaxation? What is the ultimate temperature? How exactly is the saturation of the wave linked to the onset of the heating of ions? These questions need more quantitative answers. Second, in a real reconnection problem, ions might not be very cold, and we cannot solely use electron quasi-linear theory anymore as ions make significant contribution of damping/growing of the waves. This process is very complicated and there is no theory describing it well. Therefore, smaller temperature ratio might be used in the future.

The other interesting aspect is the understanding of the electron tail and its relation to the quasi-linear change of the electron distribution function. A more quantitative model should be developed. Collisions may be added in the future to prevent these electrons to become run-away electrons.

If the physics when the external electric field is small can be well understood, further steps should

be taken to make connections with a real reconnection problem. As mentioned in section 2, the physics when the electric field is large can be quite different because the quasi-linear no longer applies. One has to take into account the nonlinear mechanisms at an early stage. Doing a simulation with large electric field requires very large electron velocity range. which means that a significant number of extra grids are needed and, therefore, make the simulation unacceptably expensive. A tricky solution is to use a truncated Maxwellian distribution function in the beginning. However, this can only help a little bit because the bulk of the distribution function will be accelerated to go beyond the velocity range when the electric field is large. Furthermore, modifying Maxwellian distribution artificially may affect the physics we are interested in. Another method that might help this is to use non-uniform grids. The idea is to make the grids denser around the resonance region and sparser in the edge. However, using non-uniform grids itself can make the simulation more expensive. The practicality of this method needs further experiments.

References

[1] V.Y. Bychenkov, V.P. Silin and S.A. Uryupin. Physics reports (Review Section of Physics Letters) 164, 3 (1988)

[2] M. Yamada, R.M. Kulsrud, and H. Ji. RMP. 82, 603 (2010)

[3] L.M. Malyshkin, T. Linde, and R.M. Kulsrud. Phys. Plasmas 12, 102902 (2005)

[4] D.A. Uzdensky. ApJ. 587:450–457 (2003)

[5] L. l Rudakov and L. V. Korablev. Soviet Physics JETP. 23, 1 (1966)

[6] L. M. Kovrizhnykh. Soviet Physics JETP. 24, 3 (1967)

[7] V.Y. Bychenkov and V.P. Silin. Zh. Eksp. Teor. Fiz. 82 (1982)

[8] R.Z. Sagdeev, Proc. Symp. Appi. Mathem. 18 (1967)

[9] D. Biskamp and R. Chodura. Phys. Rev. Lett. 27, 23 (1971).

[10] C.T. Dum, R. Chodura, and D. Biskamp. Phys. Rev. Lett. 32, 22 (1974)